

Robust Stabilization of Periodic Gaits for Quadrupedal Locomotion via QP-Based Virtual Constraint Controllers

Randall T. Fawcett^{ID}, Abhishek Pandala^{ID}, *Graduate Student Member, IEEE*,
Aaron D. Ames^{ID}, *Fellow, IEEE*, and Kaveh Akbari Hamed^{ID}, *Member, IEEE*

Abstract—This letter develops, theoretically justifies, and experimentally implements an optimization-based nonlinear control methodology for stabilizing quadrupedal locomotion. This framework utilizes virtual constraints and control Lyapunov functions (CLFs) in the context of quadratic programs (QPs) to robustly stabilize periodic orbits for hybrid models of quadrupedal robots. Properties of the proposed QP are studied wherein sufficient conditions for the continuous differentiability of the controller are presented. Additionally, this letter addresses the robust stabilization problem of the orbits based on the Poincaré sections analysis and input-to-state stability (ISS). The proposed controller is numerically and experimentally validated on the A1 quadrupedal robot with 18 degrees of freedom to demonstrate the robust stability of trotting gaits against external disturbances and unknown payloads.

Index Terms—Stability of hybrid systems, robotics, stability of nonlinear systems.

I. INTRODUCTION

LEGGED locomotion can be described by hybrid systems consisting of continuous-time domains representing the Lagrangian dynamics and discrete-time transitions representing the change of contact points with the environment [1]–[5]. Nonlinear controllers that address hybrid models of locomotion have been developed based on controlled symmetries [6], hybrid reduction [7], transverse linearization [8], and hybrid zero dynamics (HZD) [5], [9]. The HZD approach considers a set of output functions, referred to as virtual

constraints, for continuous-time domains of locomotion and asymptotically regulates them using an input-output (I-O) linearizing controller [10]. HZD controllers have been validated for whole-body motion control of underactuated bipedal robots [5], [11]–[13] and powered prosthetic legs [14], [15].

The extension of nonlinear HZD-based controllers to quadrupedal locomotion is a challenge due to its multi-contact nature. In particular, the nonlinear controllers must satisfy the feasibility of the ground reaction forces (GRFs) during different domains of locomotion. This motivates the integration of optimization-based methods with nonlinear controllers (e.g., quadratic programming (QP)-based nonlinear controllers and model predictive control (MPC)) to address the feasibility constraints. Many MPC approaches are tailored to the real-time planning of reduced-order models of locomotion, but *not* full-order models, see, e.g., [16]–[19]. In addition, one drawback of QP-based nonlinear control approaches is the possible lack of continuous differentiability (i.e., C^1) of the feedback laws with respect to the system's state [20]. Practically, the stability analysis of periodic locomotion can be checked via the eigenvalues of the Poincaré map [2], [21] which requires C^1 continuity of the feedback laws. Hence, lack of smoothness of the feedback laws prohibits the use of the powerful Poincaré sections analysis tools to study the stability of gaits.

The *overarching goal* of this letter is to present a continuously differentiable and QP-based nonlinear controller, based on virtual constraints and control Lyapunov functions (CLFs), to robustly stabilize hybrid periodic orbits for quadrupedal locomotion. The objectives and contributions of this work are as follows. We study the properties of the proposed QP-based nonlinear controller and present sufficient conditions under which the feedback laws become C^1 . We investigate conditions under which the orbit is invariant for the closed-loop hybrid system. The robust stability properties of the periodic orbit under the proposed nonlinear controller are studied via the Poincaré sections analysis and input-to-state stability (ISS). We numerically and experimentally validate the proposed nonlinear controller on the advanced A1 quadrupedal robot with 18 degrees of freedom (DOFs) to demonstrate the stability and robustness of trotting gaits against unknown payloads and external disturbances. To the best of the authors' knowledge, this is the first time a full-order HZD controller with exact feedback linearization has been implemented on quadrupedal

Manuscript received September 13, 2021; revised November 19, 2021; accepted December 1, 2021. Date of publication December 7, 2021; date of current version December 14, 2021. The work of Randall T. Fawcett was supported by the National Science Foundation (NSF) under Grant 1906727. The work of Abhishek Pandala and Kaveh Akbari Hamed was supported by the NSF under Grant 1923216. The work of Aaron D. Ames was supported by the NSF under Grant 1923239. Recommended by Senior Editor J. Daafouz. (*Corresponding author: Kaveh Akbari Hamed.*)

Randall T. Fawcett, Abhishek Pandala, and Kaveh Akbari Hamed are with the Department of Mechanical Engineering, Virginia Tech, Blacksburg, VA 24061 USA (e-mail: randallf@vt.edu; agp19@vt.edu; kavehakbarihamed@vt.edu).

Aaron D. Ames is with the Department of Mechanical and Civil Engineering, California Institute of Technology, Pasadena, CA 91125 USA (e-mail: ames@caltech.edu).

Digital Object Identifier 10.1109/LCSYS.2021.3133198

2475-1456 © 2021 IEEE. Personal use is permitted, but republication/redistribution requires IEEE permission.
See <https://www.ieee.org/publications/rights/index.html> for more information.

robots. The use of a model-based CLF for locomotion has only been validated on bipedal platforms [5], making this the first application of a model-based CLF to quadrupedal locomotion.

Our previous work [22] has used QP-based nonlinear controllers for numerical simulations of quadrupedal locomotion without studying the C^1 continuity, invariance of the orbit, and robust stability. The current work technically addresses these properties while experimentally evaluating the control framework on hardware. This work also differs from [20] and [23] in that the proposed control framework satisfies the C^1 continuity whereas the controller in [20] only meets the continuity conditions but *not* the C^1 continuity, and [23] uses the CLF condition to parameterize the rigid coupling between two subsystems for distributed control of a quadruped.

II. HYBRID MODEL OF LOCOMOTION

The objective of this section is to address hybrid dynamical models of quadrupedal locomotion. We consider floating-based models for general quadrupedal robots whose legs end at point feet. The generalized coordinates of the robot are assumed to be denoted by $q \in \mathcal{Q} \subset \mathbb{R}^{n_q}$, where \mathcal{Q} represents the configuration space for some positive integer n_q . The state vector can be taken as $x := \text{col}(q, \dot{q}) \in \mathcal{X} \subset \mathbb{R}^n$, in which $\mathcal{X} := T\mathcal{Q}$ denotes the state space with $n = 2n_q$. In addition, the joint-level torque inputs are shown by $u \in \mathcal{U} \subset \mathbb{R}^m$, where \mathcal{U} is a closed and convex admissible set of inputs for some $m < n_q$. The equations of motion can be described by the following ordinary differential equations (ODEs)

$$D(q)\ddot{q} + H(q, \dot{q}) = Bu + \sum_{\ell \in \mathcal{G}} J_\ell^\top(q) \lambda_\ell, \quad (1)$$

where $D(q) \in \mathbb{R}^{n_q \times n_q}$ denotes the positive definite mass-inertia matrix, $H(q, \dot{q}) \in \mathbb{R}^{n_q}$ represents the Coriolis, centrifugal, and gravitational terms, and $B \in \mathbb{R}^{n_q \times m}$ denotes the input matrix. In addition, \mathcal{G} represents the index set of ground contact points, $J_\ell(q) := \frac{\partial p_\ell}{\partial q}(q) \in \mathbb{R}^{3 \times n_q}$ denotes the Jacobian matrix at the contact point $\ell \in \mathcal{G}$, $p_\ell(q) \in \mathbb{R}^3$ represents the Cartesian coordinates of the contact point, and $\lambda_\ell \in \mathbb{R}^3$ is the corresponding GRF. By defining $\lambda := \text{col}\{\lambda_\ell \mid \ell \in \mathcal{G}\}$, the state equation can be expressed as

$$\dot{x} = f(x) + g(x)u + w(x)\lambda \quad (2)$$

subject to the holonomic constraints $\ddot{p} = 0$, where $p := \text{col}\{p_\ell \mid \ell \in \mathcal{G}\}$ represents the Cartesian coordinates of all contact points, which implies rigid contact and no foot slippage. More formally, we have $\ddot{p}_\ell = J_\ell(q)\ddot{q} + \frac{\partial}{\partial q}(J_\ell(q)\dot{q})\dot{q} = 0$ for all $\ell \in \mathcal{G}$. We remark that this model is valid if $\lambda_\ell \in \mathcal{FC}$ for all $\ell \in \mathcal{G}$, where $\mathcal{FC} := \{\text{col}(\lambda_x, \lambda_y, \lambda_z) \mid \lambda_z > 0, |\lambda_x| \leq \frac{\mu}{\sqrt{2}}\lambda_z, |\lambda_y| \leq \frac{\mu}{\sqrt{2}}\lambda_z\}$ denotes the friction cone for some friction coefficient μ .

Quadrupedal locomotion can be expressed by multi-domain hybrid systems. Using [2, Th. 4.3], the stability analysis of periodic orbits for multi-domain hybrid models can be reduced to that of single-domain hybrid models. In this approach, the reset map for the equivalent single-domain hybrid system can be expressed as the composition of the flows of the remaining continuous-time domains and discrete-time transitions in the order they are executed in the multi-domain hybrid systems' cycle. In particular, assuming domain 1 is the

main continuous-time domain, the equivalent reset law can be expressed as $\Delta := \Delta_{N \rightarrow 1} \circ \mathcal{F}_N \circ \dots \circ \Delta_{2 \rightarrow 3} \circ \mathcal{F}_2 \circ \Delta_{1 \rightarrow 2}$, where N denotes the number of domains and \mathcal{F}_i and $\Delta_{i \rightarrow j}$ represent the flow of the continuous-time domain i and the reset law during the discrete-time transition $i \rightarrow j$ [24], respectively, for all $i, j \in \{1, \dots, N\}$ [25, Sec. IV]. In this letter, we study periodic orbits corresponding to double-domain trotting gaits, which have left-right symmetry. Using [26, Remark 11], one can apply symmetry to the controller of domain 1 to construct the controller for domain 2. Hence, without loss of generality, we will focus on single-domain hybrid models of locomotion as follows:

$$\Sigma : \begin{cases} \dot{x} = f(x) + g(x)u + w(x)\lambda, & x \in \mathcal{X} \\ \ddot{p} = 0 \\ x^+ = \Delta(x^-), & x^- \in \mathcal{X} \cap \mathcal{S}, \end{cases} \quad (3)$$

where \mathcal{S} represents the guard of the hybrid system, referred to as the switching manifold. The state solutions of Σ undergo an abrupt change according to the C^1 reset law $x^+ = \Delta(x^-)$ when they hit the guard \mathcal{S} .

Assumption 1 (Periodic Orbit): There exists a period-one orbit \mathcal{O} for the system Σ that is transversal to the switching manifold \mathcal{S} . In particular, $\mathcal{O} := \{\varphi^*(t) \mid 0 \leq t < T\}$ for some periodic state solution $\varphi^*(t)$ and some fundamental period $T > 0$. Furthermore, the orbit intersects the switching manifold in exactly one point, i.e., $\{x^*\} := \overline{\mathcal{O}} \cap \mathcal{S}$ is a singleton, where $\overline{\mathcal{O}}$ denotes the set closure of \mathcal{O} .

III. QP-BASED NONLINEAR CONTROLLER

This section presents a nonlinear control scheme, based on QP, virtual constraints, and CLFs, for whole-body motion control and robust stabilization of the orbit \mathcal{O} . The properties of the QP-based nonlinear controller are studied to show that it becomes C^1 on an open neighborhood of the orbit.

A. Formulation of the QP-Based Nonlinear Controller

We consider a set of holonomic virtual constraints as output functions $y := h(x) \in \mathbb{R}^m$ to be imposed by the action of a feedback controller.

Assumption 2 (Output Properties): The output function $y(x)$ is assumed to be smooth (i.e., C^∞) with uniform relative degree 2 [10] with respect to the control input u in (3) on an open neighborhood of the orbit \mathcal{O} . In addition, $y(x)$ vanishes on \mathcal{O} , that is, $y(x) = 0$ for all $x \in \overline{\mathcal{O}}$.

Differentiating the output function $y(x)$ along the continuous-time dynamics (2) and setting the result equal to the desired output dynamics to solve for u yields

$$\ddot{y} = L_g L_{f_y} u + L_w L_{f_y} \lambda + L_{f_y}^2 y = -K_P y - K_D \dot{y} + v, \quad (4)$$

where “ L ” represents the Lie derivative, K_P and K_D are positive definite matrices, and $v \in \mathbb{R}^m$ is an auxiliary input. We remark that in (4), \ddot{y} is an affine function of both the inputs u and the GRFs λ , and $L_g L_{f_y}$ and $L_w L_{f_y}$ denote the corresponding decoupling matrices. The right-hand side term $-K_P y - K_D \dot{y} + v$ represents the desired output dynamics that we ultimately want to achieve by solving for (u, λ) . By defining $\eta := \text{col}(y, \dot{y}) \in \mathbb{R}^{2m}$, the output dynamics (4) can be written in a compact form as follows:

$$\dot{\eta} = \bar{f}(\eta) + \bar{g}(\eta)v := F\eta + Gv, \quad (5)$$

where

$$F := \begin{bmatrix} 0 & I \\ -K_P & -K_D \end{bmatrix} \in \mathbb{R}^{2m \times 2m}, \quad G := \begin{bmatrix} 0 \\ I \end{bmatrix} \in \mathbb{R}^{2m \times m}.$$

Since F is Hurwitz, for every positive definite $Q = Q^\top$, there exists a unique and positive definite $P = P^\top$ such that $F^\top P + P F = -Q$. A function $V_\varepsilon(\eta)$ is said to be a *rapidly exponentially stabilizing CLF (RES-CLF)* for (5) if there are positive scalars $c_1, c_2, c_3 > 0$ such that for all $0 < \varepsilon < 1$ and $\eta \in \mathbb{R}^{2m}$, the following conditions are met

$$c_1 \|\eta\|^2 \leq V_\varepsilon(\eta) \leq \frac{c_2}{\varepsilon^2} \|\eta\|^2$$

$$\inf_v \left\{ L_{\bar{f}} V_\varepsilon(\eta) + L_{\bar{g}} V_\varepsilon(\eta) v + \frac{c_3}{\varepsilon} V_\varepsilon(\eta) \right\} \leq 0. \quad (6)$$

Following [5], $V_\varepsilon(\eta) := \eta^\top P_\varepsilon \eta$ is an RES-CLF for (5) with $P_\varepsilon := \text{diag}(\frac{1}{\varepsilon} I, I) P \text{diag}(\frac{1}{\varepsilon} I, I)$. More specifically, we can show that the CLF condition can be expressed as the following affine inequality in terms of v

$$\dot{V}_\varepsilon + \frac{c_3}{\varepsilon} V_\varepsilon = \psi_0(x) + \psi_1(x) v \leq 0, \quad (7)$$

where $c_3 := \frac{\lambda_{\min}(Q)}{\lambda_{\max}(P)}$, $\psi_0(x) := \eta^\top (F^\top P_\varepsilon + P_\varepsilon F + \frac{c_3}{\varepsilon} P_\varepsilon) \eta$, and $\psi_1(x) := 2\eta^\top P_\varepsilon G$. From Assumption 2, $\eta = 0$ for all $x \in \bar{\mathcal{O}}$, and hence, the inequality (7) is reduced to the trivial case of $0 v \leq 0$ on the orbit.

Analogous to (4), the algebraic holonomic constraints arising from the stationary contacts of the stance leg ends with the ground can be expressed as

$$\ddot{p} = L_g L_{fp} u + L_w L_{fp} \lambda + L_{ff}^2 p = 0. \quad (8)$$

Assumption 3: The contact constraints are *regular* in that the square matrix $L_w L_{fp}(x)$ is full-rank for every $x \in \mathcal{X}$.

We aim to solve for (u, λ, v) that satisfy the output dynamics (4) and the contact condition (8) while addressing the CLF condition (7) as well as the feasibility constraints $u \in \mathcal{U}$ and $\lambda \in \mathcal{FC}$. For this purpose, we set up the following real-time strictly convex QP

$$\min_{(u, \lambda, v, \delta)} \frac{\gamma_1}{2} \|u\|^2 + \frac{\gamma_2}{2} \|\lambda - \lambda_d\|^2 + \frac{\gamma_3}{2} \|v\|^2 + \frac{\gamma_4}{2} \delta^2$$

$$\text{s.t. } L_g L_{fy} u + L_w L_{fy} \lambda + L_{fy}^2 y = -K_P y - K_D \dot{y} + v$$

$$L_g L_{fp} u + L_w L_{fp} \lambda + L_{fp}^2 p = 0$$

$$\psi_0 + \psi_1 v \leq \delta$$

$$u \in \mathcal{U}, \quad \lambda \in \mathcal{FC}, \quad (9)$$

where $\gamma_1, \gamma_2, \gamma_3, \gamma_4 > 0$ are weighting factors. The equality constraints of (9) correspond to the I-O linearization (4) and rigid contact assumption (8). The CLF condition (7) is then relaxed by introducing a defect variable $\delta \in \mathbb{R}$. Theorem 1 will show that this relaxation would allow the \mathcal{C}^1 continuity of the optimal solution of the QP with respect to x in an open neighborhood of the orbit $\bar{\mathcal{O}}$. The QP considers the feasibility condition of the torque inputs and GRFs as inequality constraints. The cost function finally tries to find the minimum 2-norm (minimum power) torques u that impose the actual GRFs λ to follow a desired GRF profile $\lambda_d(x)$ while reducing the magnitude of the defect variable δ and the auxiliary input v . Note that in this work, $\lambda_d = \mathbf{0}$. The existence and uniqueness of the solution to this strictly convex QP will be shown via Assumption 4 and Theorem 1.

For future purposes, the optimal solution of the QP (9) is denoted by $(u^*(x), \lambda^*(x), v^*(x), \delta^*(x))$ and is parameterized by the state vector x . Furthermore, the closed-loop hybrid system can be expressed as

$$\Sigma^{\text{cl}} : \begin{cases} \dot{x} = f^{\text{cl}}(x), & x \in \mathcal{X} \\ \dot{p} = 0 \\ x^+ = \Delta(x^-), & x^- \in \mathcal{X} \cap \mathcal{S}, \end{cases} \quad (10)$$

where $f^{\text{cl}}(x) := f(x) + g(x) u^*(x) + w(x) \lambda(x)$ is the closed-loop vector field. We remark that $\lambda(x) = \lambda^*(x)$ as from (8), $\lambda(x)$ can be uniquely computed based on $u^*(x)$.

B. Continuous Differentiability of the Feedback Controller

The QP in (9) can be expressed in a compact form as the following parameterized optimization problem

$$\mathcal{P}(x) : \begin{cases} \min_{\xi} & J(\xi, x) \\ \text{s.t.} & \rho_i(\xi, x) = 0, \quad i \in \mathcal{I}_{\text{eq}} := \{1, \dots, n_{\text{eq}}\} \\ & \omega_j(\xi, x) \leq 0, \quad j \in \mathcal{I}_{\text{ineq}} := \{1, \dots, n_{\text{ineq}}\}, \end{cases}$$

where $\xi := \text{col}(u, \lambda, v, \delta)$ represents the decision variables to be determined. The Lagrangian for $\mathcal{P}(x)$ is defined as

$$\mathcal{L}(\xi, \alpha, \beta, x) := J(\xi, x) + \sum_{i \in \mathcal{I}_{\text{eq}}} \alpha_i \rho_i(\xi, x) + \sum_{j \in \mathcal{I}_{\text{ineq}}} \beta_j \omega_j(\xi, x),$$

where α and β are the Lagrange multipliers corresponding to the equality and inequality constraints, respectively. A point $(\xi^*, \alpha^*, \beta^*)$ satisfies the *Karush-Kuhn-Tucker (KKT) conditions* for $\mathcal{P}(x_0)$ if 1) $\frac{\partial \mathcal{L}}{\partial \xi}(\xi^*, \alpha^*, \beta^*, x_0) = 0$, 2) all equality constraints are met at $(\xi, x) = (\xi^*, x_0)$, 3) all inequality constraints are satisfied at $(\xi, x) = (\xi^*, x_0)$, and 4) $\beta_j \omega_j(\xi^*, x_0) = 0$ with $\beta_j \geq 0$ for all $j \in \mathcal{I}_{\text{ineq}}$ (complementary slackness). A point $(\xi^*, \alpha^*, \beta^*)$ satisfies *strict complementary slackness* if there is not any $j \in \mathcal{I}_{\text{ineq}}$ for which both $\beta_j = 0$ and $\omega_j(\xi^*, x_0) = 0$. A point $(\xi^*, \alpha^*, \beta^*)$ is said to be *regular* if the gradients of the active constraints of $\mathcal{P}(x_0)$ are linearly independent.

The point $(\xi^*, \alpha^*, \beta^*)$ satisfies the *second-order sufficient conditions (SOSC)* of the QP $\mathcal{P}(x_0)$ if a) the KKT conditions are met, and b) the Hessian matrix meets the condition $z^\top \frac{\partial^2 \mathcal{L}}{\partial \xi^2}(\xi^*, \alpha^*, \beta^*, x_0) z > 0$ for all $z \neq 0$ such that

- 1) $z^\top \frac{\partial \rho_i}{\partial \xi}(\xi^*, x_0) = 0$ for all $i \in \mathcal{I}_{\text{eq}}$,
- 2) $z^\top \frac{\partial \omega_j}{\partial \xi}(\xi^*, x_0) = 0$ for all $j \in \mathcal{I}_{\text{ineq}}$ where $\beta_j^* > 0$,
- 3) $z^\top \frac{\partial \omega_j}{\partial \xi}(\xi^*, x_0) \leq 0$ for all $j \in \mathcal{I}_{\text{ineq}}$ where $\beta_j^* = 0$.

Assumption 4 (Optimality on the Periodic Orbit): We suppose that, for all x_0 on the orbit $\bar{\mathcal{O}}$, the QP $\mathcal{P}(x_0)$ is feasible and there exists a point $(\xi^*(x_0), \alpha^*(x_0), \beta^*(x_0))$ that satisfies the SOSC. The point $(\xi^*(x_0), \alpha^*(x_0), \beta^*(x_0))$ also satisfies the strict complementary slackness for $\mathcal{P}(x_0)$. We further suppose that the optimal control and GRFs take values in the interior of the sets \mathcal{U} and \mathcal{FC} , that is, $u^*(x_0) \in \text{int}(\mathcal{U})$ and $\lambda^*(x_0) \in \text{int}(\mathcal{FC})$, where ‘‘int’’ represents the interior of a set.

Remark 1: Assumption 4 is *not* restrictive and states that the QP has a feasible solution that satisfies the SOSC and complementary slackness for every point on the desired orbit, which follows simply from the strict convexity of the problem. It also states that the torques and GRFs corresponding to the desired trajectory remain in the interior of the feasible sets, which can be met during trajectory optimization of the desired

periodic orbit \mathcal{O} . In particular, the trajectory optimization problem for generating \mathcal{O} can be constrained by a *conservative* subset of the feasible sets \mathcal{U} and \mathcal{FC} such that the desired orbit remains in the interior of the actual feasible sets \mathcal{U} and \mathcal{FC} at all times during locomotion.

Theorem 1 (Existence, Uniqueness, and \mathcal{C}^1 Continuity of the Optimal Solution): Under Assumptions 1-4, there exist an open neighborhood of the periodic orbit \mathcal{O} , denoted by $\mathcal{N}(\mathcal{O})$, and a continuously-differentiable function $\xi^*(x) := \text{col}(u^*(x), \lambda^*(x), v^*(x), \delta^*(x))$, such that for all $x \in \mathcal{N}(\mathcal{O})$, $\xi^*(x)$ is an isolated optimal solution of the QP $\mathcal{P}(x)$.

Proof: Since $f(x)$, $g(x)$, $w(x)$, and $y(x)$ are smooth (i.e., \mathcal{C}^∞), the cost function $J(\xi, x)$ and constraints $\rho(\xi, x)$ and $\omega(\xi, x)$ are smooth in x on an open neighborhood of the orbit. In addition, $J(\xi, x)$ and constraints $\rho(\xi, x)$ and $\omega(\xi, x)$ are smooth in ξ . We next show that for all $x_0 \in \mathcal{O}$, the optimal solution of $\mathcal{P}(x_0)$, denoted by $(\xi^*, \alpha^*, \beta^*)$, satisfies the regularity condition. From Assumption 2, $\dot{y} = 0$ on the orbit. Hence, according to the output dynamics (4), the optimal v value must be zero, i.e., $v^* = 0$. Since $\psi_0 = 0$ and $\psi_1 = 0$ on the orbit, the relaxed-CLF condition in (9) is reduced to $0 \leq \delta$. According to the positive term $\frac{\gamma}{2}\delta^2$ in the cost function, we can conclude that $\delta^* = 0$. Hence, the relaxed CLF condition, which is expressed as an inequality constraint, is indeed active on the orbit. From Assumption 4, $u^* \in \text{int}(\mathcal{U})$ and $\lambda^* \in \text{int}(\mathcal{FC})$. Consequently, the feasibility constraints $u \in \mathcal{U}$ and $\lambda \in \mathcal{FC}$ of the QP (9) are inactive on the orbit. We now study the rank of the gradients of the active constraints with respect to $\xi = \text{col}(u, \lambda, v, \delta)$ that is reduced to the following matrix on the orbit

$$\begin{bmatrix} L_g L_f y(x_0) & L_w L_f y(x_0) & -I & 0 \\ L_g L_f p(x_0) & L_w L_f p(x_0) & 0 & 0 \\ 0 & 0 & 0 & -1 \end{bmatrix}. \quad (11)$$

By Assumption 3, $L_w L_f p(x_0)$ is full-rank, and hence, the gradient matrix in (11) has full row rank for every $x_0 \in \mathcal{O}$. Thus, all sufficient conditions of Fiacco's Theorem (see [27, Th. 2.1] or [20, Th. 1]) are met, resulting in the existence, uniqueness, and \mathcal{C}^1 continuity of optimal solutions of the QP on an open neighborhood of the orbit \mathcal{O} . ■

IV. ROBUST STABILITY

The objective of this section is to address the robust stabilization problem of the periodic orbit \mathcal{O} based on the Poincaré sections analysis and ISS. We consider the closed-loop hybrid model (10) subject to external disturbances during the continuous-time domain as follows:

$$\dot{x} = f^{\text{cl}}(x) + a(x)d, \quad (12)$$

where $a(x)$ is a smooth function and d is an external wrench (i.e., disturbance) defined by a finite-dimensional set of parameters [21, Sec. II.C]. Typical examples include constant disturbance inputs or splines whose parameters change from one domain to another. We suppose that $d_k \in \mathcal{D}$ represents the parameterization of the disturbance during the k -th continuous-time domain, where \mathcal{D} is a domain containing the origin. The evolution of the perturbed hybrid system on the Poincaré section \mathcal{S} can then be described by the following discrete-time

dynamics

$$x_{k+1} = \mathcal{R}(x_k, d_k), \quad k = 0, 1, \dots, \quad (13)$$

where $\mathcal{R} : \mathcal{S} \times \mathcal{D} \rightarrow \mathcal{S}$ represents the Poincaré return map parameterized by the disturbance d_k . To study the properties of the Poincaré map, we make the following assumption.

Assumption 5: We suppose that for all $x \in \mathcal{O}$, the matrix

$$T(x) := L_g L_f y - L_w L_f y (L_w L_f p)^{-1} L_g L_f p \in \mathbb{R}^{m \times m}$$

is full-rank.

Remark 2: Assumption 5 is *not* restrictive and is met inherently if the system is not overactuated. In this work, we consider a trot gait that does not have an overactuated continuous-time domain, so this assumption is satisfied. In the proof of Theorem 2, we will show that this ensures the uniqueness of the torques corresponding to the periodic gait.

Definition 1: A fixed point x^* is said to be locally ISS (LISS) for (13), if there exists $\epsilon > 0$, a class \mathcal{KL} function ϱ , and a class \mathcal{K} function ϖ such that

$$\|x_k - x^*\| \leq \varrho(\|x_0 - x^*\|, k) + \varpi(\|d\|_{l_\infty}), \quad \forall k = 0, 1, \dots,$$

for all $x_0 \in \mathcal{S} \cap \mathcal{B}_\epsilon(x^*)$ and $d \in \mathcal{B}_\epsilon(0)$, where $\mathcal{B}_\epsilon(x^*)$ and $\mathcal{B}_\epsilon(0)$ are open ϵ -neighborhood balls around x^* and 0 , respectively, and $\|d\|_{l_\infty}$ represents the l_∞ -norm.

We are now in a position to present the following theorem to investigate the existence of a fixed point and its LISS property for the Poincaré return map.

Theorem 2 (Invariance and Robust Stability): Under Assumptions 1-5, the following statements hold.

- 1) The orbit \mathcal{O} is invariant under the flow of the closed-loop hybrid system in the absence of the disturbance d . In particular, x^* is a fixed point for the Poincaré map in the absence of d , that is $\mathcal{R}(x^*, 0) = x^*$.
- 2) If the eigenvalues of $\Pi_0 := \frac{\partial \mathcal{R}}{\partial x}(x^*, 0)$ are strictly inside the unit circle, then x^* is LISS for (13).

Proof Part (1): From Assumptions 2 and 4 and the proof of Theorem 1, for every $x \in \mathcal{O}$, the QP $\mathcal{P}(x)$ is feasible and the optimal v value is zero (i.e., $v^* = 0$). Hence, the equality constraints are reduced to $L_g L_f y u + L_w L_f y \lambda + L_f^2 y = 0$ and $L_g L_f p u + L_w L_f p \lambda + L_f^2 p = 0$. Eliminating the GRFs from these equations, we can conclude that

$$T(x)u + L_f^2 y - L_w L_f y (L_w L_f p)^{-1} L_f^2 p = 0. \quad (14)$$

This, together with Assumption 5, implies that u is a unique solution for this set of equations which coincides with the open-loop control input that generates the orbit. Hence, \mathcal{O} is invariant under the flow of the closed-loop hybrid dynamics.

Part (2): Unlike [21], the closed-loop vector field is \mathcal{C}^1 , but *not* twice continuously differentiable (i.e., \mathcal{C}^2). Theorem 1 together with the transversality condition in Assumption 1 implies that $\mathcal{R}(x, d)$ is \mathcal{C}^1 with respect to (x, d) on an open neighborhood of $(x^*, 0)$. Since Π_0 is a Hurwitz matrix, for every $Q_0 = Q_0^\top > 0$, there is a unique $P_0 = P_0^\top > 0$ such that the discrete-time Lyapunov equation $\Pi_0^\top P_0 \Pi_0 - P_0 = -Q_0$ is satisfied. This shows zero-input exponential stability and thereby zero-input asymptotic stability of the fixed point x^* for the Poincaré return map. We can then conclude the desired local ISS property holds by invoking [29]. More formally, we can choose the Lyapunov function $W(x) := \delta x^\top P_0 \delta x$, where

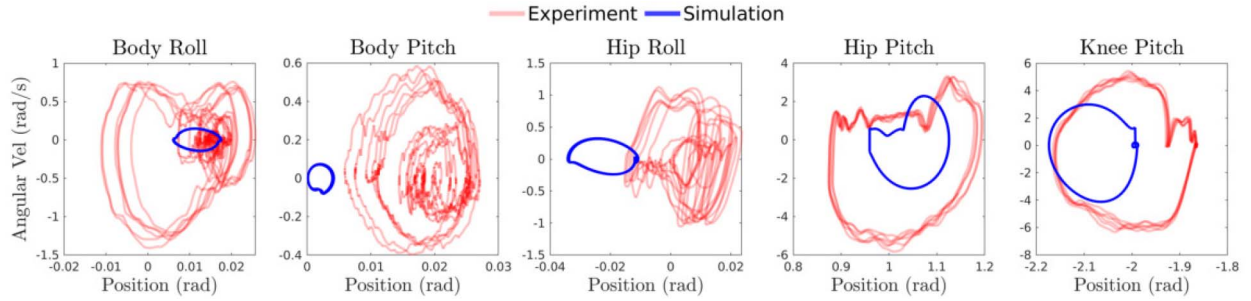


Fig. 1. Simulated and experimental data for a forward trot subject to a payload of 4.54 (kg). The joint phase plots are shown for the front right leg.



Fig. 2. This experiment displays A1 trotting under the influence of both a 4.54 (kg) payload (36% of the robot's weight) and push disturbances. The quadruped was able to resist these uncertainties and continue trotting. Videos of the experiments are available online [28].

$\delta x := x - x^*$. From [30, Lemma 2], there are $\epsilon, \zeta_0, \sigma_0 > 0$ such that for all $x \in \mathcal{S} \cap \mathcal{B}_\epsilon(x^*)$ and all $d \in \mathcal{B}_\epsilon(0) \subset \mathcal{D}$, $\Delta W := W(\mathcal{R}(x, d)) - W(x) \leq -\zeta_0 \|\delta x\|^2 + \sigma_0 \|d\|^2$. Since $\lambda_{\min}(P_0) \|\delta x\|^2 \leq W(x) \leq \lambda_{\max}(P_0) \|\delta x\|^2$, we can conclude that $W_{k+1} \leq \nu W_k + \sigma_0 \|d_k\|^2$, where $\nu := 1 - \frac{\zeta_0}{\lambda_{\max}(P_0)} < 1$. For $d = 0$, this inequality is reduced to $W_{k+1} \leq \nu W_k$, and hence, $\nu \in [0, 1)$. We can show that

$$W_k \leq \nu^k W_0 + \sigma_0 \sum_{j=0}^{k-1} \nu^{k-1-j} \|d_j\|^2 \leq \nu^k W_0 + \frac{\sigma_0}{1-\nu} d_{\max}^2,$$

where $d_{\max} := \sup_{k \geq 0} \|d_k\|$. This latter inequality together with the property $\sqrt{a+b} \leq \sqrt{a} + \sqrt{b}$ results in $\|\delta x_k\| \leq \sqrt{\frac{\lambda_{\max}(P_0)}{\lambda_{\min}(P_0)}} \|\delta x_0\| (\sqrt{\nu})^k + \sqrt{\frac{\sigma_0}{\lambda_{\min}(P_0)(1-\nu)}} d_{\max}$ for all $k = 0, 1, \dots$, which completes the proof. ■

V. NUMERICAL AND EXPERIMENTAL RESULTS

This section aims to numerically and experimentally evaluate the effectiveness of the proposed nonlinear control scheme. We consider a full-order dynamical model of the quadrupedal robot A1 made by Unitree. The floating-based model of the mechanical system consists of 18 DOFs. Six DOFs are unactuated and describe the absolute position and orientation of the robot. The remaining 12 DOFs are the actuated joints of the legs. More specifically, each leg has a 2 DOF hip joint plus a 1 DOF knee joint. The robot weighs approximately 12.45 (kg) and stands up to 0.28 (m) off the ground. In this letter, we consider a heuristic and symmetric periodic orbit \mathcal{O} for trotting at 0.1 (m/s). We remark that the orbit can also be designed via trajectory optimization techniques. The orbit satisfies Assumptions 4 and 5. We then consider 12 virtual constraints to stabilize the orbit according to Assumption 2. The first three components are defined in the Cartesian space to track the desired trajectories for the geometric center of the robot. The next three components are defined to regulate the orientation of the torso. The remaining components are defined in the Cartesian space to impose the swing leg ends

to follow the desired trajectories starting from the previous footholds and ending at the upcoming ones.

The proposed QP-based controller in (9) is solved using qpSWIFT [31] at 1kHz on an off-board laptop with an i7-1185G7 running at 3.00 GHz and 16 GB of RAM. Under nominal conditions, the computation time is 0.22 (ms) on average over the course of one domain. The QP uses $\gamma_n = \{1, 0.1, 1e6, 1e8\}$ for the weights, and assumes a coefficient of friction of $\mu = 0.7$, which results in stable locomotion.

The proposed controller was first simulated in RaiSim [32], which assumes a rigid contact model. Under nominal conditions, the controller results in stable trotting. This is further examined by subjecting the robot to push and payload disturbances that are *unknown* to the controller. Similarly, hardware experiments were performed under several disturbance conditions. The phase plots in Fig. 1 display the simulated and experimental results of a trot gait subject to a constant payload with a mass of 4.54 (kg), which is 36% of the total body mass. The gap between simulated and experimental results can be attributed to poorly modeled system dynamics, compliant feet, lack of rigorous contact and state estimation, and differences in the position of the payload. In light of these potential shortcomings, the robot is able to remain stable without knowledge of the payload. In addition to adequately handling this unmodeled payload, the robot was further able to robustly resist push disturbances during experiments without becoming unstable. Snapshots of the experiment involving both a payload and push disturbances can be found in Fig. 2 and the corresponding CLF may be found in Fig. 3. Even under these disturbances, the derivative of the CLF remains negative for nearly the entire trial, and becomes positive for only brief moments (e.g., δ remains small). It can be observed that the CLF spikes during the pushes and slowly decreases as the robot continues to step forward. Due to the hybrid nature of locomotion, convergence back to the orbit is subject to constantly changing contact domains, leading to slow recovery. Experiment videos are available online [28].

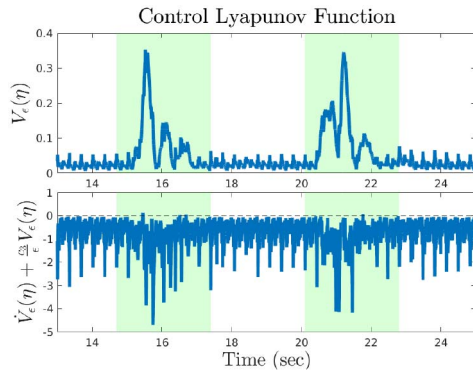


Fig. 3. CLF corresponding to the experiment in Fig. 2. The highlighted portions indicate the pushes and corresponding recovery of the robot.

VI. CONCLUSION

This letter presented a nonlinear control scheme, based on virtual constraints, CLFs, and QPs, to robustly stabilize periodic orbits for hybrid dynamical models of quadrupedal locomotion. The first theoretical contribution of this letter established sufficient conditions such that this QP-based controller is continuously differentiable on an open neighborhood of the orbit. We subsequently showed the invariance of the orbit and its robust stability via the Poincaré sections analysis and ISS. The effectiveness of the proposed controller was verified both numerically and experimentally on the A1 quadrupedal robot. The full-order and nonlinear controller was implemented on the robot as a model-based CLF-QP in real-time. The robust stability of trotting gaits against external disturbances and uncertainties arising from unknown payloads was demonstrated in practice. Future research will investigate the robustness of the gaits on rough terrains. We will also explore the integration of this control scheme with higher-level and MPC-based planning algorithms.

REFERENCES

- [1] J. Grizzle, G. Abba, and F. Plestan, "Asymptotically stable walking for biped robots: Analysis via systems with impulse effects," *IEEE Trans. Autom. Control*, vol. 46, no. 1, pp. 51–64, Jan. 2001.
- [2] E. Westervelt, J. Grizzle, C. Chevallereau, J. Choi, and B. Morris, *Feedback Control of Dynamic Bipedal Robot Locomotion*. Boca Raton, FL, USA: Taylor Francis/CRC, 2007.
- [3] H. Dai and R. Tedrake, "Optimizing robust limit cycles for legged locomotion on unknown terrain," in *Proc. IEEE 51st Annu. Conf. Decis. Control*, Dec. 2012, pp. 1207–1213.
- [4] A. M. Johnson, S. A. Burden, and D. E. Koditschek, "A hybrid systems model for simple manipulation and self-manipulation systems," *Int. J. Robot. Res.*, vol. 35, no. 11, pp. 1354–1392, 2016.
- [5] A. Ames, K. Galloway, K. Sreenath, and J. W. Grizzle, "Rapidly exponentially stabilizing control Lyapunov functions and hybrid zero dynamics," *IEEE Trans. Autom. Control*, vol. 59, no. 4, pp. 876–891, Apr. 2014.
- [6] M. Spong and F. Bullo, "Controlled symmetries and passive walking," *IEEE Trans. Autom. Control*, vol. 50, no. 7, pp. 1025–1031, Jul. 2005.
- [7] A. D. Ames, R. D. Gregg, E. D. B. Wendel, and S. Sastry, "On the geometric reduction of controlled three-dimensional bipedal robotic walkers," in *Lagrangian and Hamiltonian Methods for Nonlinear Control*. Berlin, Heidelberg: Springer, 2007, pp. 183–196.
- [8] I. Manchester, U. Mettin, F. Iida, and R. Tedrake, "Stable dynamic walking over uneven terrain," *Int. J. Robot. Res.*, vol. 30, no. 3, pp. 265–279, 2011.

- [9] E. R. Westervelt, J. W. Grizzle, and D. E. Koditschek, "Hybrid zero dynamics of planar biped walkers," *IEEE Trans. Autom. Control*, vol. 48, no. 1, pp. 42–56, Jan. 2003.
- [10] A. Isidori, *Nonlinear Control Systems*, 3rd ed. London, U.K.: Springer, 1995.
- [11] C. Chevallereau *et al.*, "RABBIT: A testbed for advanced control theory," *IEEE Control Syst. Mag.*, vol. 23, no. 5, pp. 57–79, Oct. 2003.
- [12] K. Sreenath, H.-W. Park, I. Poulakakis, and J. W. Grizzle, "Compliant hybrid zero dynamics controller for achieving stable, efficient and fast bipedal walking on MABEL," *Int. J. Robot. Res.*, vol. 30, no. 9, pp. 1170–1193, Aug. 2011.
- [13] A. E. Martin, D. C. Post, and J. P. Schmiedeler, "The effects of foot geometric properties on the gait of planar bipeds walking under HZD-based control," *Int. J. Robot. Res.*, vol. 33, no. 12, pp. 1530–1543, 2014.
- [14] R. Gregg and J. Sensinger, "Towards biomimetic virtual constraint control of a powered prosthetic leg," *IEEE Trans. Control Syst. Technol.*, vol. 22, no. 1, pp. 246–254, Jan. 2014.
- [15] H. Zhao, J. Horn, J. Reher, V. Paredes, and A. D. Ames, "Multicontact locomotion on transfemoral prostheses via hybrid system models and optimization-based control," *IEEE Trans. Autom. Sci. Eng.*, vol. 13, no. 2, pp. 502–513, Apr. 2016.
- [16] J. D. Carlo, P. M. Wensing, B. Katz, G. Bledt, and S. Kim, "Dynamic locomotion in the MIT Cheetah 3 through convex model-predictive control," in *Proc. IEEE/RSJ Int. Conf. Intell. Robots Syst. (IROS)*, Oct. 2018, pp. 1–9.
- [17] O. Villarreal, V. Barasuol, P. Wensing, and C. Semini, "MPC-based controller with terrain insight for dynamic legged locomotion," in *Proc. IEEE Int. Conf. Robot. Autom. (ICRA)*, 2020, pp. 2436–2442.
- [18] M. Chignoli and P. M. Wensing, "Variational-based optimal control of underactuated balancing for dynamic quadrupeds," *IEEE Access*, vol. 8, pp. 49785–49797, 2020.
- [19] Y. Ding, A. Pandala, C. Li, Y.-H. Shin, and H.-W. Park, "Representation-free model predictive control for dynamic motions in quadrupeds," *IEEE Trans. Robot.*, vol. 37, no. 4, pp. 1154–1171, Aug. 2021.
- [20] B. J. Morris, M. J. Powell, and A. D. Ames, "Continuity and smoothness properties of nonlinear optimization-based feedback controllers," in *Proc. 54th IEEE Conf. Decis. Control (CDC)*, 2015, pp. 151–158.
- [21] S. Veer, Rakesh, and I. Poulakakis, "Input-to-state stability of periodic orbits of systems with impulse effects via Poincaré analysis," *IEEE Trans. Autom. Control*, vol. 64, no. 11, pp. 4583–4598, Nov. 2019.
- [22] K. A. Hamed, J. Kim, and A. Pandala, "Quadrupedal locomotion via event-based predictive control and QP-based virtual constraints," *IEEE Robot. Autom. Lett.*, vol. 5, no. 3, pp. 4463–4470, Jul. 2020.
- [23] W.-L. Ma, N. Csomay-Shanklin, S. Kolathaya, K. A. Hamed, and A. D. Ames, "Coupled control Lyapunov functions for interconnected systems, with application to quadrupedal locomotion," *IEEE Robot. Autom. Lett.*, vol. 6, no. 2, pp. 3761–3768, Apr. 2021.
- [24] Y. Hurmuzlu and D. B. Marghitu, "Rigid body collisions of planar kinematic chains with multiple contact points," *Int. J. Robot. Res.*, vol. 13, no. 1, pp. 82–92, 1994.
- [25] K. A. Hamed, W. Ma, and A. D. Ames, "Dynamically stable 3D quadrupedal walking with multi-domain hybrid system models and virtual constraint controllers," in *Proc. Amer. Control Conf. (ACC)*, Jul 2019, pp. 4588–4595.
- [26] K. A. Hamed, B. Buss, and J. Grizzle, "Exponentially stabilizing continuous-time controllers for periodic orbits of hybrid systems: Application to bipedal locomotion with ground height variations," *Int. J. Robot. Res.*, vol. 35, no. 8, pp. 977–999, 2016.
- [27] A. V. Fiacco, "Sensitivity analysis for nonlinear programming using penalty methods," *Math. Program.*, vol. 10, no. 1, pp. 287–311, 1976.
- [28] *Robust Stabilization of Quadrupedal Locomotion via QP-Based Virtual Constraint Controllers*. [Online]. Available: <https://youtu.be/0A7mJvVnSn8>
- [29] C. Cai and A. R. Teel, "Characterizations of input-to-state stability for hybrid systems," *Syst. Control Lett.*, vol. 58, no. 1, pp. 47–53, 2009.
- [30] K. A. Hamed and R. D. Gregg, "Decentralized event-based controllers for robust stabilization of hybrid periodic orbits: Application to underactuated 3D bipedal walking," *IEEE Trans. Autom. Control*, vol. 64, no. 6, pp. 2266–2281, Jun. 2019.
- [31] A. G. Pandala, Y. Ding, and H.-W. Park, "qpSWIFT: A real-time sparse quadratic program solver for robotic applications," *IEEE Robot. Autom. Lett.*, vol. 4, no. 4, pp. 3355–3362, Oct. 2019.
- [32] J. Hwangbo, J. Lee, and M. Hutter, "Per-contact iteration method for solving contact dynamics," *IEEE Robot. Autom. Lett.*, vol. 3, no. 2, pp. 895–902, Apr. 2018.